# Direct and charge-exchange excitation processes in $H^+$-H (1s) collisions at 1 to 7 keV

M. Kimura*† and W. R. Thorson
*Department of Chemistry, University of Alberta, Edmonton, Alberta, Canada T6G 2G2*
(Received 16 March 1981)

We have computed direct and charge-exchange cross sections for $H^+ + H(1s) \rightarrow H^+ + H(nl)$ collisions, for projectile energies 1–7 keV, using the close-coupling method with $H_2^+$ molecular states modified by electron translation factors (ETF's); switching functions recently derived analytically for exact $H_2^+$ states were used to construct ETF corrections. Basis sets with up to 10 molecular states were used in systematic calculations, and good convergence is found for all atomic cross sections with $n \leq 2$. Results have been compared with other theoretical calculations [especially that of Crothers and Hughes (1978–1979)] and with recent experiments. Where differences between our results and those of Crothers and Hughes are found, our results agree more closely with experiment. The most notable case is the H (2s) charge-exchange (and direct) cross sections, where our results show no minimum whatever near $E = 2$–4 keV, in agreement with experiments of Morgan *et al.* (1980) and Hill *et al.* (1979), but in strong disagreement with the calculations of Crothers and Hughes and 1969 experiments of Bayfield. In one case discrepancies between our results and those of Crothers and Hughes can be shown to arise from their treatment of ETF effects (using a different switching function for the $2p\sigma_u$ state)—i.e., they obtain a much larger population of the $4f\sigma_u$ state than is found here. We have also carried out selected studies with larger basis sets (up to 16 $u$ states) to examine the behavior of cross sections for excitation to atomic levels with $n \geq 3$. These studies strongly suggest that a "ladder-climbing" sequence of excitations via upper levels is the dominant process by which ionization occurs in $H^+$-H (1s) collisions at these energies.

## I. INTRODUCTION

In the last decade, electron-transfer and excitation processes in $H^+$-H (1s) collisions at intermediate energies have been actively studied both experimentally and theoretically. The system has special theoretical interest because it provides a prototype within which a variety of important physical and methodological problems can be studied in a well-defined manner. From high energies down to intermediate energies, where projectile speed is greater than or comparable to electron orbital speeds, atomic basis coupled-state calculations may be used, while for intermediate and lower energies molecular-state expansions are more appropriate. In this paper, we report coupled molecular-state calculations on the $H^+$-H (1s) system for projectile energies in the range 1–7 keV, using a classical trajectory description of nuclear motion; up to 16 basis states have been included in the calculations, and convergence of the results as function of basis set has been studied.

Molecular-state calculations require careful consideration of the effects of electron translation factors (ETF's).[1-6] Neglect of these [as in the usual perturbed-stationary-states (PSS) scheme] introduces spurious long-range couplings and can lead to incorrect physical predictions. In this work, ETF's appropriate to molecular states, with two-center character, are described using the method of switching functions.[2,4-6] Recently, well-defined switching functions for the exact molecular states of $H_2^+$ have been deduced by an analytical two-center decomposition scheme,[7] and the resulting switching functions are in excellent agreement with those found earlier by a heuristic "optimization" procedure[6]; we have used these analytical switching functions in our computations.

Early molecular-state close-coupling studies on the $H^+$-H (1s) system were mainly concerned with resonant charge-transfer oscillations or the efficient Lyman-$\alpha$ excitation process, and employed a basis of two or at most three states ($1s\sigma_g$, $2p\sigma_u$, $2p\pi_u$).[8-12] More recent calculations using larger bases were done by Rosenthal,[13] Chidichimo-Frank and Piacentini,[14] Schinke and Krüger,[15] and Crothers and Hughes.[16] Of these, the first three studies neglect ETF effects as the PSS theory does, and hence, the results lack Galilean invariance to the choice of reference origin for electron coordinates. In addition, radial motion couplings are neglected entirely in Refs. 14 and 15.

Crothers and Hughes[16] took electron translation effects into account in their molecular-state expansion, but they did so in a manner appropriate to atomic-state bases. In an atomic-state expansion each basis orbital is attached to one of the moving nuclei and translates uniformly with it; therefore, the ETF appropriate for that orbital is uniquely and simply defined. Such a "one-center ETF" is inappropriate for a molecular state with two-center character, and especially inappropriate for symmetric systems like $H_2^+$ where

 

the molecular state have $g$ or $u$ symmetry. To avoid these difficulties, Crothers and Hughes define atomic-type fragments by forming symmetrical and antisymmetrical combinations of corresponding pairs of asymptotically degenerate $g$ and $u$ molecular states

$$\phi_{B,A} = (1/\sqrt{2})(\psi_g \pm \psi_u);$$

as internuclear separation $R \to \infty$, these become one-center functions and a one-center ETF associated with the corresponding nucleus $(B,A)$ is appropriate. After attaching such an ETF to each such fragment, Crothers and Hughes then form $g$ and $u$ basis states by recombining the modified fragments. However, the fragments $\phi_{B,A}$ defined above are not, in fact, one-center functions at finite internuclear separations, but have two-center character. To offset this deficiency, Crothers and Hughes insert a variable parameter $\lambda(R)$ in the translation factor velocity associated with the one-center fragments, and determine its optimum value at each $R$ by the Euler-Lagrange variational method.[17] In their recent paper on analytical switching functions for $H_2^+$, Thorson *et al.*[7] show that this procedure of Crothers and Hughes is equivalent, to lowest order in the velocity, to the use of a certain type of switching function. For the $1s\sigma_g$ state this "effective switching function" is surprisingly close to that which we have obtained analytically, but for the $2p\sigma_u$ state it is very different, and the coupling matrix elements obtained differ correspondingly from those used in this study, especially at distances $R \lesssim 6$–$10$ a.u.

A second defect in the calculations of Crothers and Hughes[16] is their neglect of the non-Hermitian character in the couplings between ETF-corrected molecular-basis states. When different ETF's are used for different molecular states, the resulting basis functions are no longer orthogonal (at finite $R$), and as a consequence, it can be proved that to maintain unitarity the couplings between such basis states cannot be Hermitian.[18,5] However, Crothers and Hughes retained only the Hermitian averages of the non-Hermitian couplings in their calculations. In some cases this also can lead to incorrect results for individual state cross sections.

In spite of these defects, the calculations of Crothers and Hughes[16] are based on a scheme which maintains Galilean invariance and removes spurious asymptotic couplings $(R \to \infty)$, since ETF effects are included. In most cases the results of their calculations show much closer agreement with experiment than do the earlier studies, which entirely ignore ETF effects. On the other hand, in those cases where their results disagree significantly with those we have obtained here, our results agree more closely with available recent experimental measurements.[19,20]

Our study of the $H^+$-H$(1s)$ system focusses on several different concerns: (1) agreement of theoretical predictions with available experimental results, (2) effects of ETF's on couplings between molecular states and resulting cross sections for excitation of individual states, (3) identification of the most important coupling paths leading to excitations in this system, (4) convergence of computed cross sections as a function of basis size, and (5) processes involving higher level excitations and possibly ionization.

In respect to item (1), our calculations agree well with all recent experimental measurements, usually well within stated limits of experimental error.

As far as ETF effects are concerned, we can show that ETF corrections to coupling matrix elements lead to significant effects on cross sections. In one case [the H$(2p)$ charge-transfer cross section] this can be shown to account for the improved agreement of our results with experiment (see Sec. III B). Larger effects of ETF corrections can be found for excitation probabilities of levels with $n \geq 3$.

Insofar as the detailed switching functions we have used give a correct picture of the couplings, we can identify the coupling paths for excitation of lower-lying levels in $H^+$-H$(1s)$ collisions at these energies (Fig. 4). We find, in agreement with Crothers and Hughes,[16] that the radial couplings from $2p\sigma_u$ to $3p\sigma_u$ and $4f\sigma_u$ (neglected by Refs. 14 and 15) play a significant secondary role (although our $4f\sigma_u$ excitation probabilities are much smaller than those of Ref. 16 because of major differences in the ETF's used).

We can show that good convergence of excitation probabilites and cross sections is obtained for atomic levels with $n = 2$ as the basis size is increased (see Tables II and IV), but this is not the case for higher levels. Even when detailed ETF effects are taken into account as we have done in this study, calculations with extended basis sets indicate that there are difficulties in respect to convergence and validity of close-coupling calculations for upper states employing only bound states. Even at the low energy $E = 0.7$ keV, we find that a small but not negligible portion of the total flux persistently moves to the most loosely bound molecular states included in whatever basis size we employ. We believe that this behavior may be plausibly interpreted as a crude simulation of ionizing events. In Sec. II we briefly describe methods used, and the remainder of the paper is devoted to discussion of the detailed results.

## II. DETAILED METHOD

### A. Coupled equations

We assume relative motion of the nuclei is described classically by a vector $\vec{R}(t)$, and solve the resulting time-dependent Schrödinger equation for the electron system

$$\left(H_{el}(\vec{r};\vec{R}(t)) - i\hbar\frac{\partial}{\partial t}\right)\Psi(\vec{r},t) = 0. \tag{1}$$

We expand the state vector $\Psi$ in an ETF-modified molecular basis set

$$\Psi(\vec{r},t) = \sum_n a_n(t)\phi_n(\vec{r};\vec{R}(t))\exp\left[\left(\frac{im}{2\hbar}\right)\vec{v}\cdot\vec{r}f_n(\vec{r};\vec{R})\right] \times \exp\left[-\left(\frac{i}{\hbar}\right)\int^t\left(\epsilon_n(t') + \frac{mv^2}{8}\right)dt'\right]. \tag{2}$$

Here $\vec{v} = d\vec{R}/dt$ is the relative nuclear velocity, and $\phi_n(\vec{r};\vec{R})$ are the molecular electronic eigenstates of $H_{el}$,

$$H_{el}(\vec{r};\vec{R})\phi_n(\vec{r};\vec{R}) = \epsilon_n(R)\phi_n(\vec{r};\vec{R}), \tag{3}$$

which depend parametrically upon $\vec{R}$.[21] The first exponential is a *molecular* electron translation factor (ETF), which describes motion of the electron relative to the origin of electron coordinates $\vec{r}$ due to its translation with the moving nuclei; in effect, the electron has a transport velocity $f_n(\vec{r};R)\vec{v}$ locally correlated with its position within the molecule—as is appropriate for molecular states with two-center character.[4,5] The *switching function* $f_n(\vec{r};\vec{R})$ which describes this correlation depends, in general, upon the characteristics of the bound molecular-state wave function $\phi_n(\vec{r};\vec{R})$. Recently we have derived well-defined switching functions for $H_2^+$ by an analytical two-center decomposition of the exact wave functions,[7] and we have employed these switching functions in this study.

To obtain coupled equations for the amplitudes $a_n(t)$, we substitute the expansion (2) in the Schrödinger equation, multiply the left side by $\phi_k^*(\vec{r};\vec{R})\exp[-(im/2\hbar)\vec{v}\cdot\vec{r}f_k(\vec{r};\vec{R})]$, and integrate over electron coordinates $\vec{r}$. For the collision energies considered here it is an adequate approximation to expand the ETF's in powers of the velocity $\vec{v}$, retaining only the terms up through order $\vec{v}^2$ in the coupled equations [we also neglect terms in the acceleration $(d\vec{v}/dt)$]. Then it can be shown that the resulting *close-coupled equations* are

$$\begin{aligned}
i\hbar\dot{a}_k(t) = &\sum_{n\neq k}\vec{v}\cdot(\underline{P}+\underline{A})_{kn}a_n(t)\exp\left[-\left(\frac{i}{\hbar}\right)\int^t(\epsilon_n-\epsilon_k)dt'\right] \\
&+\sum_n\left[\left(\frac{im}{\hbar}\right)\left(\left\langle k\left|[\vec{v}\cdot(\vec{s}_n-\vec{s}_k)]\right\{\vec{v}\cdot\left[-i\hbar\vec{\nabla}_R+\left(\frac{im}{\hbar}\right)[H_{el},\vec{s}_n]\right]\right\}\right|n\right\rangle\right. \\
&\qquad\left.-\sum_j\langle k|[\vec{v}\cdot(\vec{s}_j-\vec{s}_k)]|j\rangle\left\langle j\left|\vec{v}\cdot\left[-i\hbar\vec{\nabla}_R+\left(\frac{im}{\hbar}\right)[H_{el},\vec{s}_n]\right]\right|n\right\rangle\right) \\
&\qquad+\langle k|(m/8)[(f_n^2-1)\vec{v}^2+(\vec{v}\circ\vec{r})^2(\vec{\nabla}_r\cdot f_n\vec{r})^2+2(\vec{v}\cdot\vec{r})(f_n\vec{v}\cdot\vec{\nabla}_r f_n+2\vec{v}\cdot\vec{\nabla}_R f_n)]|n\rangle\Big]a_n \\
&\times\exp\left[-\left(\frac{i}{\hbar}\right)\int^t(\epsilon_n-\epsilon_k)dt'\right],
\end{aligned} \tag{4}$$

where

$$\underline{P}_{kn} = \langle k|-i\hbar\vec{\nabla}_R|n\rangle, \tag{5}$$

$$\underline{A}_{kn} = (im/\hbar)\langle k|[H_{el},\vec{s}_n]|n\rangle = (im/\hbar)(\epsilon_k-\epsilon_n)\langle k|\vec{s}_n|n\rangle, \tag{6}$$

and

$$\vec{s}_n = \tfrac{1}{2}f_n(\vec{r};\vec{R})\vec{r}. \tag{7}$$

In these equations, the matrix elements denoted by Dirac brackets are evaluated using the *unmodified* molecular states

$$|n\rangle = \phi_n(\vec{r};\vec{R}). \tag{8}$$

For low to intermediate collision energies, the dominant terms in Eqs. (4) are those first-order in $\vec{v}$; $\underline{P}$ is the usual nonadiabatic coupling matrix encountered in (uncorrected) PSS theory, while $\underline{A}$ represents the corrections to these couplings due to ETF effects.[4,5] The messy remaining terms in Eqs. (4), all of order $\vec{v}^2$, are small except at the higher energies we studied where they can have a maximum effect of ~15% on some cross sections; where significant, we have retained them. It can be shown that Eqs. (4) conserve probability to within errors of order $(\vec{v})^3$; in this connection, the non-Hermitian character of coupling matrices like $\underline{A}$, and some of the $\vec{v}^2$ terms, is a required property and should *not* be destroyed by taking Hermitian averages (as was done in a similar context by Crothers and Hughes[16]).

For the range of collision energies considered,

it is an adequate approximation for $\vec{R}(t)$ to use either constant-velocity or Coulomb trajectories, and we tested this by comparing results obtained with each at $E = 1.0$ keV (below 1.0 keV, Coulomb trajectories should be used because of effects on rotational couplings in united-atom manifolds[11]).

Since the collision Hamiltonian is rigorously centrosymmetric, the state vector (2) is composed of noninteracting $g$ and $u$ components and there are corresponding sets of $g$ and $u$ close-coupled equations (4). If the index "1" designates the initial state in each set ($1s\sigma_g$ or $2p\sigma_u$, respectively), the initial condition for Eqs. (4) (corresponding to "proton $A$ plus atom $B$") is

$$a_k(-\infty) = (1/\sqrt{2})\delta 1k \tag{9}$$

and (for given energy $E$ and each impact parameter $\rho$) the final-state amplitudes $a_k(+\infty;\rho)$ are computed. We integrated Eqs. (4) numerically, using the method of Bulirsch and Stoer,[22] with a relative truncation error automatically maintained between $10^{-4}$ and $10^{-5}$.

For many purposes it is useful to define the probability of excitation to *molecular state* $k$,

$$P_k(E,\rho) = |a_k(+\infty;\rho)|^2, \tag{10a}$$

and the corresponding integrated cross section

$$Q_k(E) = 2\pi \int_0^\infty \rho d\rho P_k(E,\rho). \tag{10b}$$

However, to compute probabilities and cross sections for excitation to specific *atomic states* ($j$), atomic state amplitudes $b_j(+\infty;\rho)$ must first be formed by an appropriate coherent addition of molecular-state amplitudes, before using Eqs. (10):

$$b_j(+\infty;\rho) = e^{i\gamma} \sum_k C_{jk} a_k(+\infty;\rho) \times \exp\left[-\left(\frac{i}{\hbar}\right)\int_{-\infty}^{\infty} (\epsilon_k(t') - \epsilon_j^0)dt'\right] \tag{11}$$

($\gamma$ is an arbitrary phase). The coherences considered in Eqs. (11) are of the following two types:

(a) "*Direct*" and "*charge-exchange*" excitation amplitudes are formed by addition and/or subtraction of the (Schrödinger picture) amplitudes for matching pairs of $g$ and $u$ molecular states. For the incident channel, where final amplitudes are significant for both $u$ and $g$ components, the well-known resonant charge-exchange oscillations result. For the excited channels, on the other hand, amplitudes for excitation of $g$ molecular states are small below ~ 5 keV, with the result that the direct and charge-transfer cross sections are nearly the same.

(b) In a hydrogenic ion or atom where atomic levels like $2s$ and $2p$ are essentially degenerate, the molecular states are asymptotically correlated not to atomic eigenstates but to the "hybrid" (Stark-field) states which diagonalize the polarizing field produced by the other nucleus. For the $n = 2$ level in $H_2^+$, for example, the pairs of molecular states ($2s\sigma_g$, $3d\sigma_g$) and ($3p\sigma_u$, $4f\sigma_u$) correlate to $g$ and $u$ "$sp$ hybrids" and this mixing must also be unscrambled to obtain $2s$ and $2p_0$ amplitudes.

### B. Molecular eigenstates

Exact molecular eigenstates and eigenvalues $\epsilon_n(R)$ were generated by the method of Bates and Carson[23,24]; the solutions are separable in prolate spheroidal coordinates ($\xi, \eta, \phi$),

$$\phi_n(\vec{r};\vec{R}) = X(\xi)S(\eta)\Phi(\phi), \tag{12}$$

where

$$X(\xi) = (\xi^2-1)^{|m|/2} e^{-\alpha\xi}(\xi+1)^\sigma \sum_j c_j \left(\frac{\xi-1}{\xi+1}\right)^j, \tag{13a}$$

$$S(\eta) = \sum_l f_l P_l^{|m|}(\eta), \tag{13b}$$

$$\Phi(\phi) = (2\pi)^{-1/2} e^{\pm im\phi}. \tag{13c}$$

Parameters in Eqs. (13) are defined in Refs. 23 and 24. Matrix elements involving these functions were evaluated by Gauss-Legendre and Gauss-Laguerre quadratures with relative errors less than $1\times10^{-6}$.

To study convergence with basis-set size, we have done systematic calculations with sets of 4, 8, and 10 molecular states, as listed in Table I. In addition, some selected calculations have been done with as many as 16 $u$ states. Figure 1 shows potential-energy curves $\epsilon_n(R)$ for the ten $H_2^+$ states considered in systematic studies.

TABLE I. Molecular basis sets for systematic close-coupling calculations.

| Number of states | Gerade basis states | Ungerade basis states | Limiting atomic states |
|---|---|---|---|
| 4 | $\|1s\sigma_g\rangle$<br>$\|3d\pi_g\rangle$ | $\|2p\sigma_u\rangle$<br>$\|2p\pi_u\rangle$ | $1s$<br>$2p_1$ |
| 8 | 2 above, plus<br>$\|3d\sigma_g\rangle$<br>$\|4d\pi_g\rangle$ | 2 above, plus<br>$\|3p\sigma_u\rangle$<br>$\|3p\pi_u\rangle$ | $2s + 2p_0$<br>$3p_1$ |
| 10 | 4 above, plus<br>$\|2s\sigma_g\rangle$ | 4 above, plus<br>$\|4f\sigma_u\rangle$ | $2s + 2p_0$ |

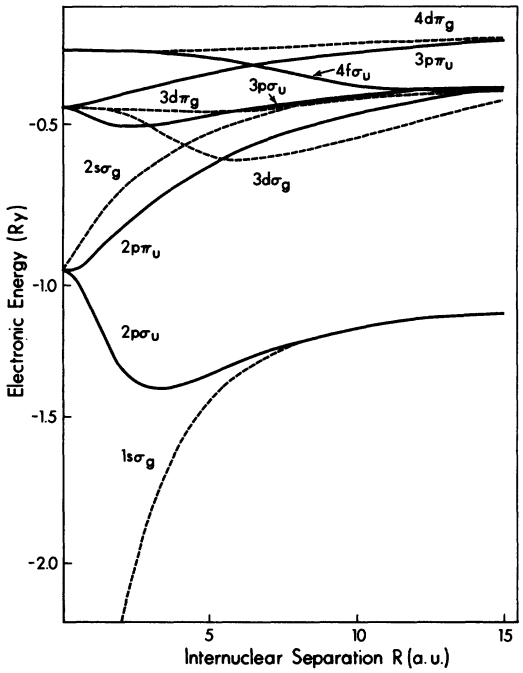


FIG. 1. Electronic potential-energy curves $\epsilon_n(R)$ vs $R$, for ten states of $H_2^+$.

### C. Couplings and matrix elements

The couplings $\vec{\nabla}\cdot(\underline{P}+\underline{A})$ may be divided into *radial* and *angular* parts,

$$\vec{\nabla}\cdot(\underline{P}+\underline{A})_{kn}=\dot{R}(P^R+A^R)_{kn}+R\dot{\theta}(P^\theta+A^\theta)_{kn}. \quad (14)$$

Here

$$P^R_{kn}=\left\langle k\left|-i\hbar\left(\frac{\partial}{\partial R}\right)\right|n\right\rangle, \quad (15a)$$

$$P^\theta_{kn}=-R^{-1}\langle k|\hat{L}_y|n\rangle, \quad (15b)$$

are the usual uncorrected coupling matrix elements appearing in PSS theory; $\hat{L}_y$ is the electronic orbital angular momentum component perpendicular to the collision plane, relative to the geometric center, and in (15a) the derivative is taken keeping $\vec{r}$ fixed with respect to this point. To evaluate (15a) we used the Hellmann-Feynman relation

$$-i\hbar\left\langle k\left|\left(\frac{\partial}{\partial R}\right)_{\vec{r}}\right|n\right\rangle=-i\hbar(\epsilon_n-\epsilon_k)^{-1}\left\langle k\left|\left(\frac{\partial H_{el}}{\partial R}\right)_{\vec{r}}\right|n\right\rangle. \quad (15c)$$

The ETF corrections are

$$A^R_{kn}=(im/\hbar)(\epsilon_k-\epsilon_n)\langle k|zf_n(\vec{r};R)|n\rangle \quad (16a)$$

and

$$A^\theta_{kn}=(im/\hbar)(\epsilon_k-\epsilon_n)\langle k|xf_n(\vec{r};R)|n\rangle, \quad (16b)$$

where $z$, $x$ are, respectively, parallel and perpendicular to $\vec{R}$.

### D. Asymptotic coupling in the 2s-2p manifold

In the asymptotically degenerate atomic $(2s, 2p)$ manifold, rotational and radial couplings give rise to a long-range coupling problem which it is convenient to treat separately. The three molecular states involved for the $u$ system are $(2p\pi_u, 3p\sigma_u, 4f\sigma_u)$ and for the $g$ system $(3d\sigma_g, 3d\pi_g, 2s\sigma_g)$. The two hybrid $sp\,\sigma$ states are linked by Coriolis coupling to the $\pi$ state, and to each other by radial coupling. Since both couplings and splittings decrease only as $R^{-2}$, neither $R$ nor $t$ is a suitable progress variable. We found that for $R \geq 15$ a.u. we could describe both couplings and splittings accurately by analytical models based on atomic states, and by using the action variable

$$\eta=\int_\infty^t \frac{\rho v_0 dt'}{R^2}$$

as a progress variable we can solve the asymptotic coupling problem very efficiently. In effect its solution may be represented as a three-state propagator $U(\infty;R_0)$ which converts molecular-state amplitudes at $R_0$ to those at $R\to\infty$; this is attached to the output from the integration over the interior "real collision" region. We used this device to generate amplitudes for all *three* final molecular states, even in those cases where the basis used in the interior region did not span all those states [e.g., in the eight-state basis of Table I, $4f\sigma_u$ and $2s\sigma_g$ do not appear in the close-coupling problem, but amplitudes for these states at $R\to\infty$ are fed from amplitudes in the other components $(2p\pi_u, 3p\sigma_u)$ and $(3d\sigma_g, 3d\pi_g)$ at $R=R_0$]. Effects of the asymptotic coupling are small but not negligible and should be taken into account to give correct predictions of atomic $2s$, $2p_0$, and $2p_{\pm1}$ excitation probabilities.

We estimate that for all the cross sections we have computed, the numerical precision of values given is at least 0.1% (i.e., errors of at most ±1 in the third significant digit). Excitation probabilities (including the data in Table IV) have somewhat smaller precision errors. These precision errors are much less than the known sources of error arising from straightline vs Coulomb trajectories (at lower energies) or from third- and higher-order terms in the velocity, neglected in the coupled equations (4) (at higher energies).

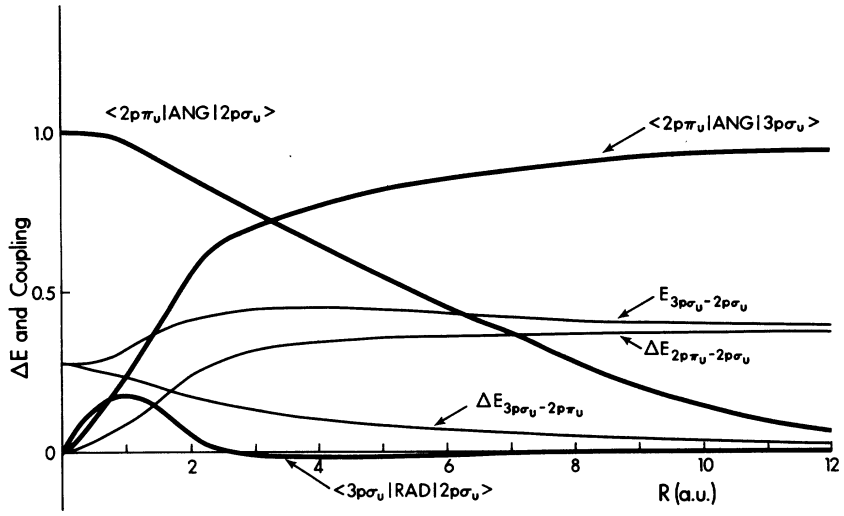


FIG. 2. Prominent radial and angular coupling matrix elements and corresponding energy separations vs $R$ for $u$ manifold.

## III. RESULTS

### A. Couplings and excitation probabilities

Figures 2 and 3 show some of the more prominent couplings and associated energy gaps. For $H^+$-H ($1s$) collisions in the energy range considered, the strong $2p\sigma_u$-$2p\pi_u$ rotational coupling associated with united-atom orbital degeneracy is the main source of excitations, and excitations from the entire $g$ manifold, or from $2p\sigma_u$ via radial coupling, are less important. Thus, for example, a good qualitative picture for the $3p\sigma_u$ excitation is the two-step process $2p\sigma_u \rightarrow 2p\pi_u \rightarrow 3p\sigma_u$. However, the radial $2p\sigma_u \rightarrow 3p\sigma_u$ coupling is not negligible, and at higher energies it plays an important, if secondary, part in the $3p\sigma_u$ excitation and resulting atomic ($2s$, $2p_0$) cross sections.

In the $g$ manifold, the most significant couplings from $1s\sigma_g$ are radial $1s\sigma_g \rightarrow 3d\sigma_g$ and angular $1s\sigma_g \rightarrow 3d\pi_g$, but due to the large energy gaps neither is very effective except at the higher energies studied. Which initial process is more important depends sensitively on both energy and impact

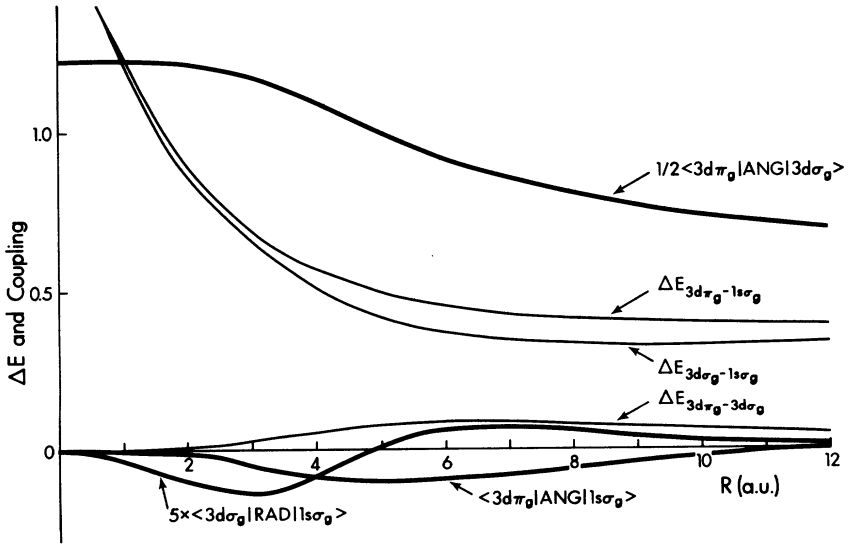


FIG. 3. Prominent radial and angular coupling matrix elements and corresponding energy separations vs $R$ for $g$ manifold.

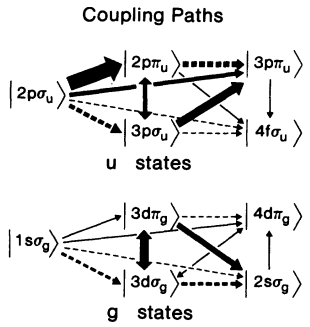


FIG. 4. Effective couplings and excitation paths for $u$ and $g$ manifolds in $H^+$-H (1$s$) collisions (0–7 keV). ——→: Angular coupling, - - - →: radial coupling; thickness of connecting arrow indicates qualitative importance.

parameter, but in any case there is subsequent strong $3d\sigma_g \leftrightarrow 3d\pi_g$ mixing due to the strong rotational coupling between them. Because the $g$-manifold's contribution to overall excitation processes is small, we will focus most of our detailed discussion on the $u$ components.

We have earlier discussed the long-range couplings among the degenerate atomic ($2s, 2p$) components. Figure 4 depicts the main pathways for excitation of the five lowest molecular states of each parity; the thickness of the connecting arrows indicates the effective coupling strengths.

We should emphasize that the description taken for electron translation factors has very significant effects on the coupling matrix elements, and this is especially so for some of the secondary couplings. As an important instance, Fig. 5 shows our matrix elements for the couplings $2p\sigma_u \leftrightarrow 4f\sigma_u$ and $2p\pi_u \leftrightarrow 4f\sigma_u$, compared with those used by Crothers and Hughes[16] (Hermitian averages). These authors's much larger matrix elements for coupling to $4f\sigma_u$ lead, at the higher energies studied, to very different predictions from ours for the atomic state ($2p_0, 2p_{\pm1}$) populations and resulting polarization of Lyman-$\alpha$ emission (cf. Sec. IIIB). Even larger errors in couplings and excitation probabilities result if ETF effects are neglected entirely—as was done by most previous authors[13-15] except Crothers and Hughes.

Except for asymptotic couplings within degenerate atomic manifolds (see Sec. IID), most couplings are of reasonably short range after ETF corrections are taken into account. For more highly excited states, however, we find that there are certain groups of couplings which fall off very slowly ($\sim R^{-2}$ asymptotically) because of very large distortion effects on the diffuse orbitals involved. A prominent sequence of such couplings is the radial $\pi$-$\pi$ couplings (e.g., $2p\pi_u \rightarrow 3p\pi_u$, $4p\pi_u$, $5p\pi_u, \ldots$; $3p\pi_u \rightarrow 4p\pi_u$, $5p\pi_u, \ldots$, etc.), which have an important effect on higher level excitations (see Sec. IIIC).

Figure 6 shows molecular-state excitation probabilities vs impact parameter at 5 keV for the

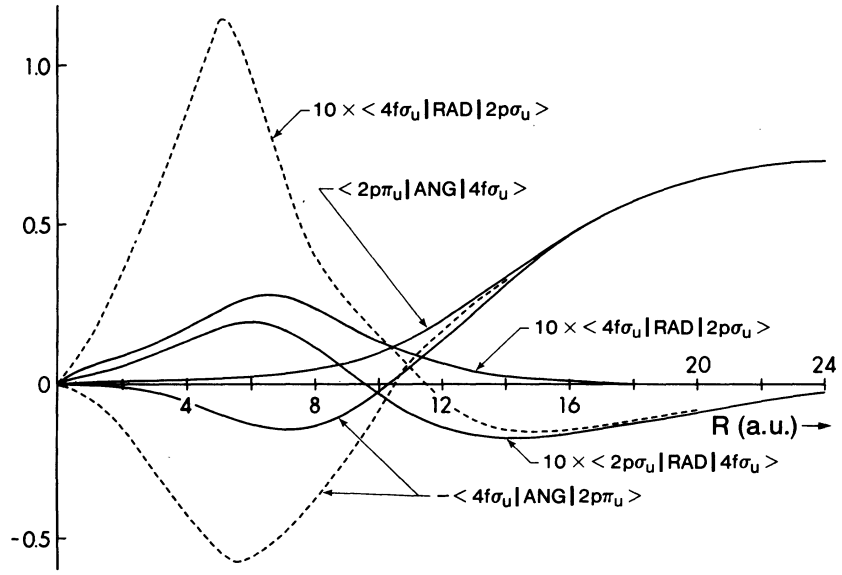


FIG. 5. Coupling matrix elements linking $2p\sigma_u$, $2p\pi_u$ states to the $4f\sigma_u$ state as computed with analytically determined switching functions (solid curves—note non-Hermitian character), and as computed by Crothers and Hughes, Ref. 16 (dashed curves—Hermitian average).

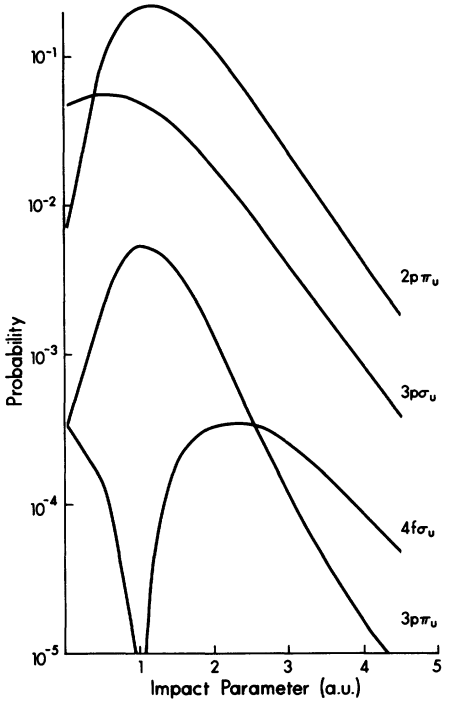


FIG. 6. Probabilities for excitation of molecular states vs impact parameter at 5 keV. Angular and radial couplings included.

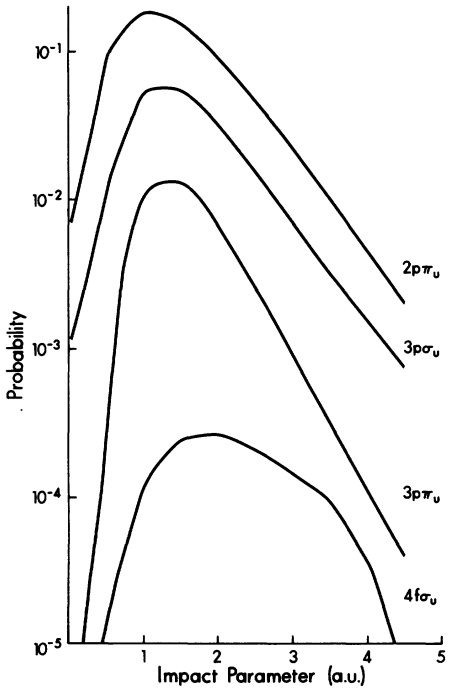


FIG. 7. Same as Fig. 6, but only angular couplings included.

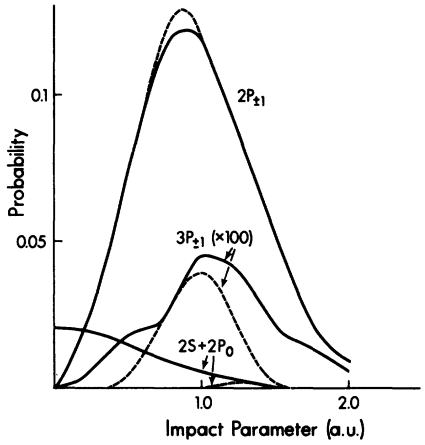


FIG. 8. Atomic-state excitation probabilities vs impact parameter at $E=1$ keV. Solid curves: present work; dashed curves: results of Schinke and Krüger, Ref. 15 (angular couplings only, no ETF corrections).

five-$u$-state basis; the importance of radial couplings is illustrated clearly by comparison with Fig. 7, which shows the same data when only angular couplings are included. The most obvious effect of radial coupling is the change in the $3p\sigma_u$ excitation probability, especially at small impact parameters, due to the direct excitation $2p\sigma_u \rightarrow 3p\sigma_u$. A secondary effect is the decrease (by a factor of ~5) in the $3p\pi_u$ probability when radial coupling is included; this occurs because $3p\pi_u$ amplitude, which is produced at small $R$ by angular coupling from $3p\sigma_u$ ($2p\pi_u \rightarrow 2p\sigma_u \rightarrow 2p\pi_u$), returns to $2p\pi_u$ late in the collision when radial couplings are included. The effect of direct radial coupling $2p\sigma_u \rightarrow 4f\sigma_u$ can also be seen, though it is much smaller.

The effects of radial coupling are also very evident in Fig. 8, which compares atomic-state transition probabilities vs impact parameter at 1 keV, for $2p_{\pm1}$, $2s+2p_0$, and $3p_{\pm1}$, with the results of Schinke and Krüger[15] who neglected radial couplings as well as the ETF corrections. From these results we can see that there is no theoretical justification for ignoring the radial couplings; although their matrix elements are smaller, they act effectively over a wider range of distances and impact parameters.

Figures 9 and 10 show the "histories" of collisions for the five-$u$-state basis at $E=5$ keV and $\rho=0.5$ and 5 a.u., respectively. Again the effect of radial coupling in populating $3p\sigma_u$ (in advance of $2p\pi_u$) is evident, with the subsequent excitation of $3p\pi_u$ by rotational coupling at small $R$. The effects of the couplings $3p\pi_u \rightarrow 4f\sigma_u$, $3p\pi_u \rightarrow 2p\pi_u$ during the outgoing part of the trajectory can also be seen.

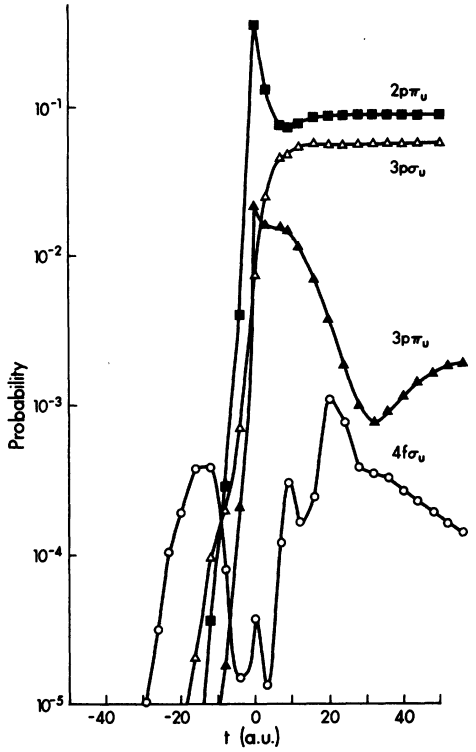


FIG. 9. Collision history [molecular-state probabilities vs time (a.u.)] for $E=5$ keV, impact parameter 0.5 a.u.

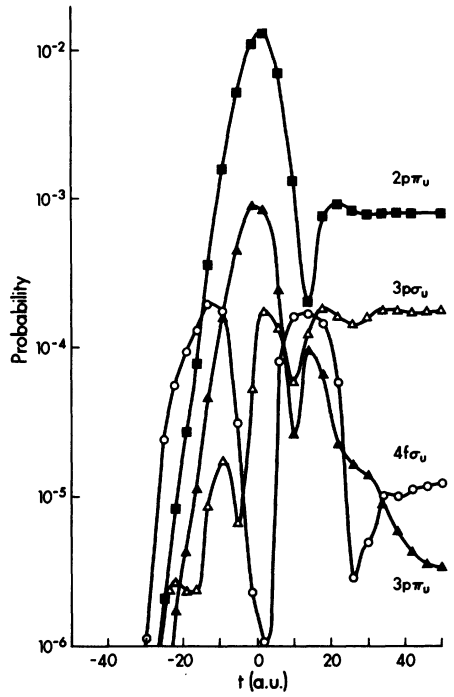


FIG. 10. Collision history [molecular-state probabilities vs time (a.u.)] for $E=5$ keV, impact parameter 5.0 a.u.

### B. Cross sections

Direct and charge-exchange excitation cross sections for atomic $2s$ and $2p$ states, as well as the resonant charge transfer to $H(1s)$, have been computed for projectile energies 1–7 keV, for the various basis sets used.

Our results for the integrated total charge-transfer cross section as function of energy are in good agreement with other molecular-state calculations and with experiment for the energy range studied, and we have not presented them here. Figure 11 shows the differential charge-exchange cross section (all states) at $E=1$ keV, and is again in reasonably good agreement with experiment[25,26] and other theoretical calculations,[12,15,16] especially that of Crothers and Hughes.[16]

Figure 12 compares our results for the $H\,2p$ charge-exchange cross section $(2p_0+2p_{\pm1})$ with those of Schinke and Krüger[15] and Crothers and Hughes,[16] and with experimental values found by Morgan, Geddes, and Gilbody.[27] (For $2p$ excitation, the $g$-manifold contribution is relatively small; direct and charge-exchange cross sections differ by less than 8% over the range studied.)

The agreement between our results and the experimental values is very good, except at the highest energies shown. The success of molecular-state descriptions in predicting at least quali-

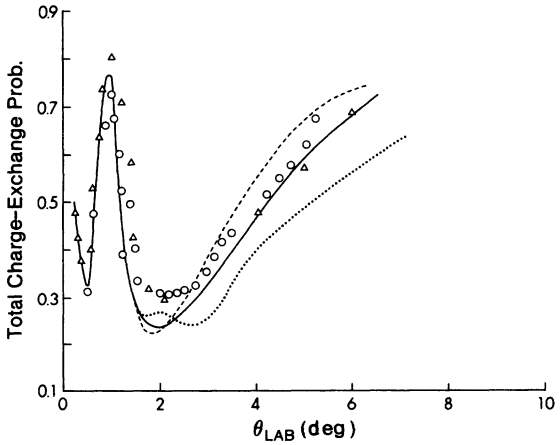


FIG. 11. Charge-exchange probability (all states) vs laboratory-scattering angle (Coulomb deflection) at $E=1$ keV. ——: Present work; -----: Ref. 15, Schinke *et al.*; · · · · · : Ref. 14, Piacentini *et al.* Results of Crothers and Hughes (Ref. 16), not shown, nearly coincide with ours. Experimental data are ○: Ref. 26; △: Ref. 27.

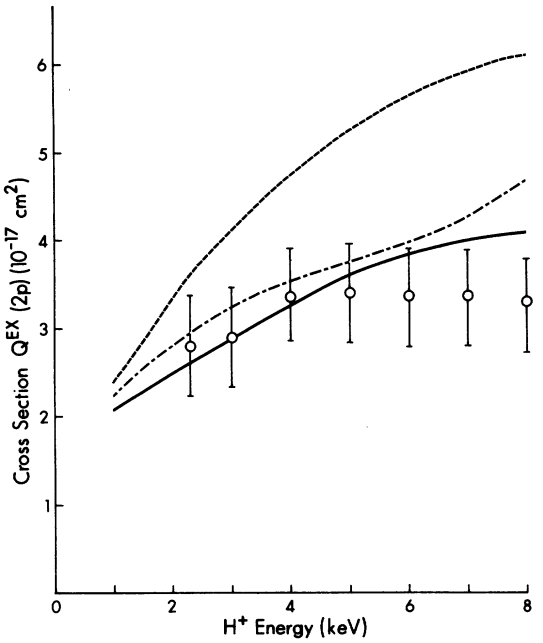


FIG. 12. Charge-exchange cross section for H ($2p$) (all components) vs $E$. ——: Present work; —·—·—: Crothers and Hughes; -----: Schinke and Krüger. ○: Experimental data of Morgan *et al.*, Ref. 27.

tatively the correct behavior for this cross section confirms that they are appropriate at these energies; atomic-state basis calculations (not shown) give much larger cross sections which vary rapidly at low energies, although inclusion of pseudostates causes marked improvement in the results.

The discrepancy between our results and those of Schinke and Krüger[15] for this cross section can be shown to arise mainly from the neglect of ETF corrections. [The curve shown for their results was constructed by addition of their published curves for $2p_{\pm1}$ and for $2s$ (equal to $2p_0$ in their calculation).] At 5 keV, for example, more than 90% of their total $2p$ cross section arises from $2p_{\pm1}$ excitation via angular coupling from the initial $2p\sigma_u$ state. As Crothers and Hughes also point out,[16] the uncorrected $2p\sigma_u - 2p\pi_u$ coupling matrix element behaves in a completely incorrect way for $R \gtrsim 3$ a.u., due to the presence of the linearly increasing moment arm in the operator $\hat{L}_y$. At energies 2 keV and above, calculations show that the resulting spurious coupling leads to the much larger $2p\pi_u$ excitation probabilities found by Schinke and Krüger.

The results of Crothers and Hughes[16] for the $2p$ cross section are in close agreement with ours up to $E \approx 6$ keV, and then show a rapid increase relative to ours and to the experimental values. Calculations, as well as comments of Crothers and Hughes,[16] indicate that this increase is due to the larger $4f\sigma_u$ populations resulting from their much larger $2p\sigma_u - 4f\sigma_u$ and $2p\sigma_u - 4f\sigma_u$ coupling matrix elements (cf. Fig. 5) and this in turn is a direct result of their ETF description.

Using the formula of Percival and Seaton,[28] we have also calculated the polarization of Lyman-$\alpha$ emission. Since our excitation cross sections for $2p_{\pm1}$ are much larger than those for $2p_0$ over the entire energy range considered, negative values are obtained as follows: −0.247 at 1 keV, −0.212 at 3 keV, −0.166 at 5 keV, and −0.140 at 7 keV. These disagree with polarizations computed by Crothers and Hughes,[16] which become positive between 4 and 5 keV; the sign change in their results is directly attributable to the much larger $4f\sigma_u$ excitation probabilities they predicted due to their description of ETF effects.

Cross sections for direct and charge-exchange excitation to the $2s$ atomic state are shown in Figs. 13 and 14. Effects of $1s\sigma_g - 3d\sigma_g$ and other $g$-manifold couplings play some role at higher energies so we find that $Q^D_{2s}$ and $Q^{ex}_{2s}$ are slightly different. For charge exchange, our results agree rather well with the recent data of Morgan, Stone, and Mayo[19] and of Hill, Geddes, and Gilbody[20] from 1.5 to 6 keV (although Hill *et al.* give somewhat larger values than those of Morgan *et al.* below 3 keV). On the other hand, our results differ very substantially from those reported by Crothers and Hughes,[16] which show a

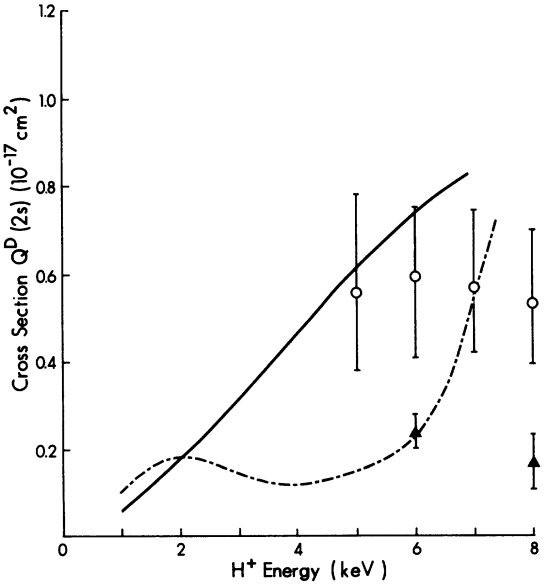


FIG. 13. Direct excitation cross section H ($2s$) vs $E$. ——: Present work; —·—·—: Crothers and Hughes. Experimental data are ○: Morgan *et al.*, Ref. 27; ▲: Chong and Fite, Ref. 29.

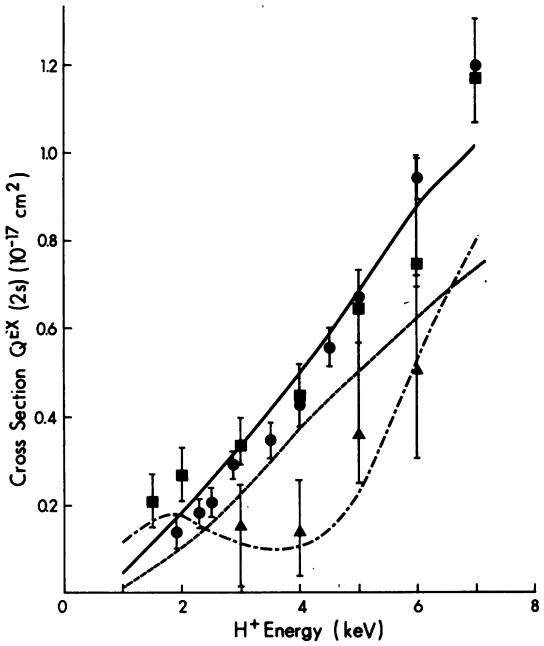


FIG. 14. Charge-exchange cross section for H(2$s$) vs $E$. ——: Present work; —·—·—: Crothers and Hughes; -----: Schinke and Krüger. Experimental data are ●: Morgan *et al.*, Ref. 19; ■: Hill *et al.*, Ref. 20; ▲: Bayfield, Ref. 31.

pronounced minimum near 3–4 keV. This result of Crothers and Hughes is similar to results found in some atomic basis-set calculations (not shown)[32] and appears to follow closely the older experimental values reported by Bayfield.

In an effort to determine the origin of this and other discrepancies between our results and those of Crothers and Hughes,[16] we have carried out close-coupling calculations using the same ten-state basis (to first order in velocity only, and using straightline trajectories), but employing the matrix elements shown in their papers for $E=2$, 3, 4, and 5 keV. For all *except* the 2$s$ excitation cross sections, we have obtained good qualitative agreement with their published curves. For example, the 2$p$ excitation cross sections we obtain from these calculations differ from their reported values by at most +20% (at 5 keV) and follow the same monotonic trend; the discrepancy is probably attributable to the corrections of second order in velocity, which are included in their values, and which should increase uniformly with increasing collision energy. In the case of the 2$s$ cross sections, however, we have not been able to reproduce their results even qualitatively; the results we obtained from these calculations lie 30–40% above our curves shown in Figs. 13 and 14, and show no sign of any dip or even a marked change in slope. We therefore cannot prove that this large discrepancy results from the different treatment of ETF effects given by Crothers and Hughes.[16]

Figure 14 also shows the results for the 2$s$ charge-exchange cross section reported by Schinke and Krüger[15]; the results found by Chidichimo-Frank and Piacentini[14] (not shown) are very similar. There is a substantial discrepancy between our results and these, which is masked to some extent by the linear plot used for Fig. 14; at 1 keV our value is at least 4 or 5 times larger than that of Schinke and Krüger,[15] and at 5 keV, it is still about 40% larger. As is shown by comparison of Figs. 6 and 7 (5 keV), our larger cross sections result from inclusion of the radial couplings, especially $2p\sigma_u - 3p\sigma_u$, leading to a higher population of the $3p\sigma_u$ level at smaller impact parameters. Figure 8 (1 keV) shows that this effect is enhanced still more at lower energies. Given the limits of error on the experimental values reported in Refs. 19 and 20, we cannot be certain that these unambiguously confirm our higher values, especially at the lower energies, but they do tend to agree much more closely with our results than with those of Schinke and Krüger.[15]

In Table II the convergence of $n=2$ excitation cross sections as a function of basis size is

TABLE II. Charge-exchange cross sections (cm$^2$) showing convergence vs basis size at $E=1$, 3, and 5 keV.

| $E$ (keV) | 1 | | 3 | | 5 | |
|---|---|---|---|---|---|---|
| Atomic states | $2p_{\pm1}$ | 2$s$ | $2p_{\pm1}$ | 2$s$ | $2p_{\pm1}$ | 2$s$ |
| Four-state basis | $2.00\times10^{-17}$ | | $2.42\times10^{-17}$ | | $2.92\times10^{-17}$ | |
| Eight-state basis | 1.98 | $0.653\times10^{-18}$ | 2.40 | $3.90\pm10^{-18}$ | 2.87 | $8.23\times10^{-18}$ |
| Ten-state basis | 1.98 | 0.637 | 2.39 | 3.64 | 2.86 | 7.06 |

TABLE III. Molecular basis sets ($u$ states only) for upper-state excitation-convergence studies.

| Number of $u$ states | Basis states | Atomic principal quantum number |
|---|---|---|
| 8 | $\|2p\sigma_u\rangle$; | 1 |
| | $\|2p\pi_u\rangle$, $\|3p\sigma_u\rangle$, $\|4f\sigma_u\rangle$; | 2 |
| | $\|2p\pi_u\rangle$, $\|4f\pi_u\rangle$, $\|4p\pi_u\rangle$; | 3 |
| | $\|4p\pi_u\rangle$; | 4 |
| 14 | 8 above, plus | |
| | $\|4f\delta_u\rangle$, $\|5f\sigma_u\rangle$ | 3 |
| | $\|5f\pi_u\rangle$, $\|5p\sigma_u\rangle$, $\|5f\delta\rangle$ | 4 |
| | $\|5p\pi_u\rangle$ | 5 |
| 16 | 14 above, plus | |
| | $\|6f\pi_u\rangle$ | 5 |
| | $\|6p\pi_u\rangle$ | 6 |

examined, for the basis sets of Table I. In each case the $2p_{\pm1}$ cross section has clearly converged; for the $2s$ cross section, though the change from eight to ten basis states is fairly small, effects of further increase in the basis would deserve further study.

### C. Convergence studies

To explore further the convergence properties of a close-coupling calculation on this system, we increased the size of the $u$ basis by adding more highly excited molecular states strongly coupled to those already considered, and performed calculations of molecular-state excitation probabilities at selected energies and impact parameters. In addition to the five-state basis already considered, we used bases with 8-, 14-, and 16-$u$ states. Table III lists these states and the corresponding atomic-state manifolds to which they dissociate.

As these Rydberg states are very loosely bound and closely spaced in energy, they can hardly be expected to behave even approximately in adiabatic fashion. Moreover, the coupling matrix elements linking them, both radial and angular, are of very long range and reflect the very large polarizabilities of these states. Even at the low end of the energy range we considered it has proved impossible to obtain reasonable convergence of excitation probabilities for atomic levels $n \geq 3$. Moreover, as the basis size is increased a significant portion of the flux moves up to the highest levels accessible; a collision history diagram shows that this is occurring in the outgoing portion of the collision trajectory and is due to the long-range $\pi_u - \pi_u$ couplings in particular. Table IV indicates the size of the effects in question, for $E = 0.7$ keV and three impact parameters.

Since close-coupling molecular-state calculations as currently performed include only bound states which "follow" the nuclei, they make no allowance for flux loss due to ionization.[36] However, as was pointed out by Thorson and Levy,[33] it is physically unreasonable to regard a state as "bound" in a collision, if the transport kinetic energy of the electron, relative to the other collision partner, is comparable to or greater than the static binding energy; events corresponding in a tightly bound state to charge exchange will lead in such a case to ionization. At $E = 0.7$ keV, levels with $n \gtrsim 5$ fall in this category. This suggests that a significant portion of the probability listed in Table IV for the higher levels (including $n = 4$) *corresponds in reality to ionizing events*.

Some years ago an adiabatic perturbation theory of direct impact ionization[33] was developed in this laboratory and used by SethuRaman, Thorson, and Lebeda[34] to compute ionization from the close-coupled $1s\sigma_g$, $2p\sigma_u$, and $2p\pi_u$ molecular states of $H_2^+$ for projectile energies $\leq 1$ keV. The

TABLE IV. Total excitation probabilities for atomic level $n$ [$E = 0.7$ keV, $|2p\sigma_u\rangle$ initial state ($n_0 = 1$); impact parameters 1, 2, and 3 a.u.].

| Impact parameter in (a.u.) | Basis size | $n=2$ | $n=3$ | $n=4$ | $n=5$ | $n=6$ |
|---|---|---|---|---|---|---|
| 1 | 8 | $2.406\times10^{-1}$ | $2.141\times10^{-2}$ | $1.341\times10^{-3}$ | | |
| | 14 | $2.324\times10^{-1}$ | $1.762\times10^{-2}$ | $3.791\times10^{-3}$ | $1.230\times10^{-4}$ | |
| | 16 | $2.351\times10^{-1}$ | $1.239\times10^{-2}$ | $2.237\times10^{-3}$ | $1.738\times10^{-4}$ | $1.335\times10^{-4}$ |
| 2 | 8 | $1.588\times10^{-2}$ | $8.010\times10^{-4}$ | $1.018\times10^{-4}$ | | |
| | 14 | $1.498\times10^{-2}$ | $6.732\times10^{-4}$ | $1.029\times10^{-3}$ | $1.354\times10^{-5}$ | |
| | 16 | $1.595\times10^{-2}$ | $5.978\times10^{-4}$ | $2.903\times10^{-4}$ | $2.303\times10^{-5}$ | $1.550\times10^{-5}$ |
| 3 | 8 | $1.175\times10^{-4}$ | $5.506\times10^{-5}$ | $7.616\times10^{-7}$ | | |
| | 14 | $1.001\times10^{-4}$ | $4.176\times10^{-5}$ | $6.354\times10^{-6}$ | $8.862\times10^{-6}$ | |
| | 16 | $1.131\times10^{-4}$ | $2.500\times10^{-5}$ | $2.103\times10^{-6}$ | $1.915\times10^{-5}$ | $2.391\times10^{-6}$ |

physical assumption in these calculations is that ionization dominantly occurs by a single impulsive excitation from a tightly bound level to the continuum. Recently, Choi and Thorson[35] have repeated these calculations using a more accurate evaluation of the collision trajectory integrals, and obtained results which, though somewhat smaller, are *of the same order of magnitude* as those found by SethuRaman *et al.* At 0.7 keV and impact parameter 1.0 a.u., the resulting $u$ impact ionization probabilities are 50–100 times *smaller* than the aggregates for $n=5$ and 6 listed in Table IV, and drop off much more rapidly with increasing impact parameter than those in Table IV.

We may tentatively conclude from this that (a) even in this primitive system the dominant mechanism for ionization does *not* involve direct excitation by a single impulse, but a ladder-climbing process in which the electron is gradually detached in a series of small impulses, and does not come out with large amounts of excess energy; and (b) if excitation to higher principal quantum levels above $n=2$, or perhaps 3 at most, in these systems is to be computed reliably, close-coupling calculations need to come to grips with the description of flux loss due to ionization, even at quite low energies.

## ACKNOWLEDGMENTS

We thank the Natural Sciences and Engineering Research Council of Canada for support of this research through Operating Grant No. A-5330. Computations were done on the Amdahl V/7 digital computer at the Computing Centre, University of Alberta.

---

*Present address: c/o Dept. of Physics, University of Missouri, Rolla, Missouri 65401.

†Based on a doctoral thesis submitted by M. Kimura in partial fulfillment of requirements for the Ph.D. degree, University of Alberta, 1981.

[1]D. R. Bates and R. McCarroll, Proc. R. Soc. London Ser. A 245, 175 (1958); Adv. Phys. 11, 39 (1962).
[2]S. B. Schneiderman and A. Russek, Phys. Rev. 181, 311 (1969).
[3]A. Riera and A. Salin, J. Phys. B 9, 2877 (1976).
[4]W. R. Thorson and J. B. Delos, Phys. Rev. A 18, 117 (1978); 18, 135 (1978).
[5]J. B. Delos and W. R. Thorson, J. Chem. Phys. 70, 1174 (1979).
[6]J. Rankin and W. R. Thorson, Phys. Rev. A 18, 1990 (1978).
[7]W. R. Thorson, M. Kimura, J. H. Choi, and S. K. Knudson, Phys. Rev. A 24, 1768 (1981).
[8]A. F. Ferguson, Proc. R. Soc. London Ser. A264, 540 (1961).
[9]F. J. Smith, Proc. Phys. Soc. London 84, 889 (1964).
[10]D. R. Bates and D. A. Williams, Proc. Phys. Soc. London 83, 425 (1964).
[11]S. K. Knudson and W. R. Thorson, Can. J. Phys. 48, 313 (1970).
[12]R. McCarroll and R. D. Piacentini, J. Phys. B 3, 1336 (1970).
[13]H. Rosenthal, Phys. Rev. Lett. 27, 635 (1971).
[14]U. C. Chidichimo-Frank and R. D. Piacentini, J. Phys. B 7, 548 (1974).
[15]R. Schinke and H. Krüger, J. Phys. B 9, 2469 (1976).
[16]D. S. F. Crothers and J. G. Hughes, Proc. R. Soc. London Ser. A 359, 345 (1978); Philos. Trans. R. Soc. London 292, 56 (1979).
[17]M. E. Riley and T. A. Green, Phys. Rev. A 4, 619 (1971).
[18]T. A. Green, Proc. Phys. Soc. London 86, 1017 (1965).
[19]T. J. Morgan, J. Stone, and R. Mayo, Phys. Rev. A 22, 1460 (1980).
[20]J. Hill, J. Geddes, and H. B. Gilbody, J. Phys. B 12, L341 (1979).
[21]If electron coordinates are described in a nonrotating reference frame, then $H_{el}(\vec{r};\vec{R})$ and its eigenfunctions $\phi_n$ depend parametrically on the vector $\vec{R}$, not merely on its magnitude; this viewpoint is formally useful (cf. Ref. 5).
[22]R. Bulirsch and J. Stoer, Numerische Mathematik 8, 1 (1966).
[23]D. R. Bates and T. R. Carson, Proc. R. Soc. London Ser. A 234, 207 (1956).
[24]J. Rankin, Ph.D. thesis, University of Alberta, Edmonton, 1978 (unpublished).
[25]J. C. Houver, J. Fayeton, and M. Barat, J. Phys. B 7, 1358 (1974).
[26]H. F. Helbig and E. Everhart, Phys. Rev. 140, 1715 (1965).
[27]T. J. Morgan, J. Geddes, and H. B. Gilbody, J. Phys. B 6, 2118 (1973).
[28]I. C. Percival and M. J Seaton, Philos. Trans. R. Soc. London Ser. A 251, 113 (1958).
[29]Y. P. Chong and W. L. Fite, Phys. Rev. A 16, 933 (1977).
[30]T. G. Winter and N. F. Lane, Phys. Rev. A 17, 66 (1978); T. G. Winter and G. J. Hatton, *ibid.* 21, 793 (1980); G. J. Hatton, N. F. Lane, and T. G. Winter, J. Phys. B 12, L571 (1979).
[31]J. E. Bayfield, Phys. Rev. 185, 105 (1969).
[32]D. Rapp and D. Dinwiddie, J. Chem. Phys. 57, 4919 (1972); D. Rapp, D. Dinwiddie, D. Storm, and T. E. Sharp, Phys. Rev. A 5, 1290 (1972). See also, I. M. Cheshire, D. F. Gallagher, and A. J. Taylor, J. Phys. B 3, 813 (1970).
[33]W. R. Thorson and H. Levy II, Phys. Rev. 181, 232 (1969); H. Levy II and W. R. Thorson, *ibid.* 181, 244 (1969).
[34]V. SethuRaman, W. R. Thorson, and C. F. Lebeda, Phys. Rev. A 8, 1316 (1973).
[35]J. H. Choi and W. R. Thorson (private communication; unpublished).
[36]Inclusion of pseudostates in a basis set may incorporate virtual effects of the continuum but does not describe ionization flux loss.